BNL-229425-2026-JAAM

Design and fabrication of a four-rod radio frequency quadrupole with a variable aperture

S. Ikeda, T. Kanesue

To be published in "Nuclear Instruments and Methods in Physics Research Section A: Accelerators, Spectrometers, Detectors and Associated Equipment"

May 2026

Collider Accelerator Department

Brookhaven National Laboratory

U.S. Department of Energy

USDOE Office of Science (SC), Basic Energy Sciences (BES)

DISCLAIMER

Nuclear Instruments and Methods in Physics Research A 1085 (2026) 171303

Contents lists available at ScienceDirect

Nuclear Inst. and Methods in Physics Research, A

journal homepage: www.elsevier.com/locate/nima

Design and fabrication of a four-rod radio frequency quadrupole with a variable aperture

Shota Ikeda [a,*], Shunsuke Ikeda [b], Takeshi Kanesue [b], Toshiro Sakabe [b], Antonino Cannavo [b], Masahiro Okamura [b], Kazumasa Takahashi [c], Chuan Zhang [d], Masashi Masuoka [e], Horana Gamage Madhawa [f]

[a] Institute of Science Tokyo, Japan
[b] Brookhaven National Laboratory, United States
[c] Nagaoka University of Technology, Japan
[d] GSI Helmholtz Center for Heavy Ion Research, Germany
[e] TIME Co., Ltd, Japan
[f] Columbia University, United States

A B S T R A C T

Radiofrequency quadrupole (RFQ) linear accelerators with variable aperture cell parameters offer an effective means of accelerating high-intensity ion beams exceeding 100 mA and have been implemented in various RFQ designs. However, in a four-rod RFQ, the use of dielectric perturbation methods to measure the voltage distribution behind the rod electrodes is not applicable when implementing variable aperture geometries, because changes in the rod shape influence the electric field at the location of the perturbation element. Therefore, it was necessary to design the rod profile for each cell such that the electric field distribution behind the rods remains unaffected by changes in the aperture. In this study, we present a method to adjust the voltage distribution by modifying the geometry of the rod electrodes according to each cell's aperture parameters. This design approach enables the integration of variable aperture cells into a four-rod RFQ linac, significantly enhancing the achievable beam current. To ensure uniform capacitance and maintain a constant rod-electrode voltage despite variations in the average aperture radius, we developed a systematic method for shaping the rod electrodes. This method was refined using two-dimensional (2D) and three-dimensional (3D) electromagnetic field simulations to optimize the electrode cross-sectional profiles. The fabricated rod electrodes were then installed in a four-rod RFQ, and the electric field distribution was measured using the perturbation method and tuned by adjusting the base plates. As a result, the measured variation of ±1.1 % confirms that this design methodology can produce a sufficiently uniform voltage distribution for high-current beam acceleration. These results demonstrate the practical feasibility of a variable-aperture four-rod RFQ linac.

1. Introduction

A radio-frequency quadrupole linear accelerator (RFQ linac) uses an RFQ electric field to focus and accelerate low-energy ion beams. The RFQ linac processes DC ion beams at several tens of keV/u and accelerates them to higher energies with efficient transmission. These linacs serve as injectors for larger accelerator systems and have also been used as standalone accelerators for compact accelerator-driven neutron sources and particle-induced X-ray emission (PIXE) [1,2]. In an RFQ linac, several resonance structures are employed depending on the required operating frequency. For example, a four-vane RFQ linac features vane electrodes connected to a cavity resonator operating in the TE_{211} mode. Consequently, the resonant frequency of a four-vane RFQ typically exceeds 100 MHz, making it suitable for accelerating light ions such as protons and deuterons [3]. Conversely, when the resonant frequency is below 100 MHz, a four-rod RFQ linac is commonly used. This design consists of a resonator with multiple stem electrodes mounted on a base plate, to which four rod electrodes are attached. The operating mode is the π mode, with an RF phase shift of approximately half a wavelength between adjacent stems. As a result, the four-rod RFQ linac maintains a moderate physical size and operates efficiently at resonance frequencies below 100 MHz; therefore, it is primarily used for accelerating heavy ions.

RFQ linacs have been studied and developed to accelerate high-intensity ion beams in response to the expanding range of ion-beam applications. As a result, hydrogen ion beams (proton or H− beams) with currents exceeding 50 mA have been successfully accelerated at the Los Alamos National Laboratory [4], Brookhaven National Laboratory (BNL) [5], and CERN LINAC2 [6]. More recently, LINAC4 at CERN, J-PARC in Japan [7], and the Spallation Neutron Source (SNS) at Oak

* Corresponding author.
E-mail address: ikeda.s.a793@m.isct.ac.jp (S. Ikeda).

https://doi.org/10.1016/j.nima.2026.171303
Received 27 October 2025; Received in revised form 6 January 2026; Accepted 20 January 2026
Available online 21 January 2026

Ridge National Laboratory [8] have achieved acceleration of H− beams with currents of several tens of milliamperes. These beams are subsequently injected into synchrotrons to produce high-intensity proton beams, which serve as drivers for applications such as particle physics experiments, spallation neutron production, and muon production. Regarding heavy-ion beam acceleration, UNILAC at GSI accelerates a 12 emA U4+ beam using a 36.136 MHz IH-RFQ linac followed by a 108 MHz Alvarez-type drift-tube linac (DTL) [9]. At BNL, the pre-injector system consists of a laser ion source, an electron beam ion source, a 100.625 MHz four-rod RFQ linac, and an IH-DTL, enabling acceleration of heavy-ion beams with a mass-to-charge ratio of 6.25 at a beam current of 5 emA for RHIC and NSRL operations [10]. In addition, at IMP, a 53.667 MHz four-rod RFQ linac for heavy ions has been developed, and continuous-wave (cw) operation has successfully accelerated heavy-ion beams with a current of approximately 200 μA [11].

A laser ion source (LIS) is a device in which a solid target is irradiated with a pulsed laser at an intensity of 10^8 W/cm^2 or higher, producing an ion beam extracted from the resulting ablation plasma. The laser energy is absorbed by the target, rapidly increasing its temperature and inducing a phase transition to a gaseous or plasma state. The ablation plasma expands adiabatically and drifts perpendicular to the target surface, generating a high-intensity ion beam with low emittance. The beam pulse width produced by the LIS is directly proportional to the drift distance of the ablation plasma, whereas the beam current density is inversely proportional to the cube of the drift distance.

High-intensity and highly charged heavy-ion beams can be generated using a LIS. However, transporting these beams through a conventional low-energy beam transport system and injecting them into an RFQ linac is difficult due to strong space–charge effects. To address this issue, a direct plasma injection scheme (DPIS) was proposed as a method for injecting high-intensity heavy-ion beams directly into an RFQ linac, and its proof of principle was demonstrated in 2000 [12]. A four-rod RFQ linac designed for high-intensity heavy-ion acceleration using DPIS successfully accelerated C^{4+} ion beams exceeding 40 mA [13]. Furthermore, the installation of a solenoid guide providing magnetic fields of several hundred gauss in the drift region between the laser ion source and the RFQ linac reduced the divergence of the expanding laser ablation plasma, thereby enabling extension of the ion-beam pulse length [14]. More recently, a compact accelerator-driven neutron source based on an inverse-kinematics scheme using a lithium beam was proposed, in which the DPIS–LIS and RFQ linac successfully accelerated a 35 mA Li^{3+} beam [15].

The space–charge effect in charged particle beams becomes more pronounced at higher beam currents and lower energies. As a result, acceleration of heavy-ion beams in the 100 mA class has remained challenging, because the focusing strength of conventional RFQ linacs is often insufficient to suppress beam divergence.

In an RFQ, the phase advance of the beam depends on both the transverse focusing strength B and the defocusing term arising from space–charge forces. The transverse focusing strength depends on the inter-vane voltage V, the aperture radius r, and the RF frequency f, and is approximately given by

$$B \propto \frac{V}{r^2 f^2} \tag{1}$$

indicating that the focusing strength scales inversely with the square of the aperture radius r. As the beam propagates through the RFQ, the space–charge force varies significantly from the injection region through the bunching and acceleration stages. When the focusing strength B is kept constant, a mismatch between the transverse and longitudinal phase advances occurs, leading to emittance growth.

On the other hand, to efficiently accelerate protons and deuterons above 100 mA, variable aperture cell parameters are proposed in an RFQ linac [16,17]. This acceleration method mitigates the increase in emittance caused by space–charge effects by introducing a cell parameter that continuously adjusts the average aperture radius based on the beam's longitudinal position. By introducing a variable-aperture compensation, the aperture radius is adjusted cell-by-cell so that the focusing strength B is appropriately modified to maintain the ratio of transverse to longitudinal phase advance close to unity. This suppresses emittance growth and enables stable acceleration of high-current beams. For example, an RFQ linac incorporating this method was developed at J-PARC and successfully accelerated proton beams [18]. In variable-aperture RFQs, the capacitance of each cell changes with the average aperture radius along the beam's longitudinal direction. Therefore, adjusting the voltage between the electrodes was necessary for each cell. In a four-vane RFQ linac, the inductance is modified by continuously adjusting the thickness of the vane electrodes to match the required voltage between the electrodes in each cell [19].

In contrast to four-vane RFQs, the metallic-sphere perturbation technique cannot be directly applied to four-rod RFQ structures. Instead, measurements of the inter-electrode voltage distribution rely on placing a dielectric perturbing object behind the rod electrodes, using the base plate as a reference. However, this measurement approach becomes unreliable when variable-aperture geometries are introduced, because modifications to the rod-electrode shape also affect the electric field at the probe location. To address this issue, the rod geometry must be designed individually for each cell such that the electric field behind the rods remains invariant against changes in the aperture. By maintaining a constant electric field at the perturbation site, conventional dielectric-based field measurement methods can still be applied for axial field tuning.

In this study, we propose a design method for four-rod RFQ linacs that achieves a uniform inter-electrode voltage distribution across all cells by maintaining electric-field invariance through local capacitance compensation. This approach ensures a consistent inter-electrode voltage even with variable-aperture cell parameters. The proposed method enables the practical implementation of variable-aperture designs in four-rod RFQs and has the potential to significantly enhance the beam current of accelerated heavy ions.

This study presents a method for designing a variable-aperture four-rod RFQ based on electromagnetic field simulations, as well as the fabrication of rod electrodes developed using this method and the associated low-power RF measurements performed with a four-rod RFQ linac. The paper is organized as follows. Section 1 describes the challenges associated with accelerating high-intensity heavy-ion beams using RFQ linacs and introduces the concept of a variable-aperture four-rod RFQ. Section 2 presents the design methodology and simulation results for the variable-aperture four-rod RFQ linac. Section 3 describes the fabrication of the RFQ based on the design results and its low-power RF measurements. Finally, Section 4 summarizes the conclusions of this study.

2. Design of a variable aperture four-rod RFQ linac

The main parameters of the variable-aperture four-rod RFQ linac are

Table 1
Beam parameters of the four-rod variable-aperture RFQ linac.

Resonant frequency	100 MHz
Accelerated particle	$^7Li^{3+}$
Peak beam current	≧100 emA
Input energy	21.8 keV/u
Output energy	320 keV/u
Horizontal normalized rms emittance	0.33 → 0.85
Vertical normalized rms emittance	0.33 → 0.90
Number of cells	138
Rod length	1997.5 mm
Inter-vane voltage(V)	105 kV
r_0(without RMS)	6.2–7.8 mm
Transverse vane-tip curvature	Variable (≦1.0r_0)
E_{max} (Kilpatrick factor)	≦22.3 MV/m (1.96)

listed in Table 1, and the corresponding cell parameters are shown in Fig. 1. These parameters were designed based on the concepts of variable aperture and constant-voltage cell parameters [20] in order to maximize the accelerated heavy-ion beam current. To accelerate the Li^{3+} beam, a laser ion source can readily generate fully stripped ions in the 100 mA class. Therefore, the beam acceleration tests for this RFQ linac are planned to be conducted in a low-duty pulsed mode (below 0.1 %). The maximum extraction voltage of the ion source is approximately 50 kV, corresponding to an injection energy of 21.8 keV/u. The rod electrodes have a total length of 1997.5 mm and are designed to accelerate Li^{3+} ions to 320 keV/u. Beam dynamics simulations using PARMTEQM show that, when 200 emA of Li^{3+} ions are injected into the RFQ linac, 148.8 emA are accelerated, corresponding to a transmission efficiency of 74.4 %. The average aperture radius, excluding the radial matching section (RMS), ranges from 6.2 to 7.8 mm along the longitudinal direction. The inter-electrode voltage is set to 105 kV, resulting in a maximum field strength per cell of up to 22.3 MV/m (Kilpatrick factor = 1.96).

As part of the design process for the rod electrodes in a variable-aperture four-rod RFQ linac, the cross-sectional shape of the rod electrodes was determined based on two-dimensional electromagnetic field simulations [21]. Subsequently, a three-dimensional model of the rod electrodes was generated from the optimized 2D cross sections, and electromagnetic field analyses were performed using three-dimensional simulation software. As shown in Fig. 1, although the inter-electrode voltage is kept constant, the average aperture radius decreases from the inlet to the outlet of the RFQ. Under these cell parameters, a rod-electrode geometry that provides uniform capacitance in each cell is required to achieve a uniform voltage distribution along the structure. Therefore, lateral adjustment of the rod-electrode cross-sectional shape is necessary to ensure uniform capacitance throughout the variable-aperture cells.

2.1. Design of the rod electrode cross-sectional shape using 2D electromagnetic field simulation

The four-rod RFQ linac can be modeled as a series of coupled LC circuits, in which current flows from the base plate through the stem electrodes on both sides, each providing inductance. Capacitance is formed between the rod electrodes connected to the stems. The current flowing through the stem electrodes charges the rods and generates an electric field between them. When the region between two adjacent stem electrodes is regarded as a single LC resonant circuit, the capacitance, resonant frequency, and inter-electrode voltage are related as given by Eq. (2) [22].

$$V_n = J_n / f C_n \tag{2}$$

where C_n and V_n denote the capacitance and inter-vane voltage of the rod electrodes between adjacent stem electrodes, respectively, J_n is the current flowing between the stems, and f is the resonant frequency of the four-rod RFQ linac. Even though the average aperture radius varies from cell to cell, the circuit can be treated equivalently by designing the rod electrodes to provide uniform capacitance across all cells.

The complex cross-sectional geometry of the rod electrodes makes direct calculation of the cell capacitance difficult. To overcome this difficulty, the two-dimensional electromagnetic field simulation code RFQFISH was employed to evaluate the effective capacitance for each cell. RFQFISH is capable of modeling the two-dimensional electromagnetic field distribution and resonant frequency of a four-vane RFQ structure. For this type of resonant structure, the vane-tip capacitance C, the inductance of the cavity walls L, and the resonant frequency f are related by Eq. (3).

$$f = 1 \Big/ 2\pi\sqrt{LC} \tag{3}$$

When the resonant frequency is kept constant, the capacitance C remains unchanged for a given inductance, even if the average aperture diameter varies.

In the RFQFISH analysis, the vane tips of a four-vane RFQ were used as an equivalent cross section of a rod electrode in order to evaluate the resonant frequency, after which the capacitance of the rod-electrode cross section was adjusted accordingly (right panel of Fig. 2). To establish a reference geometry, the cross-sectional configuration of a four-vane RFQ resonating at 100 MHz was first simulated, as shown in Fig. 2. In this analysis, the electrode tip was modeled with a rod-like profile while maintaining the same average aperture radius as that used in the BNL RFQ for Li^{3+} ion acceleration [15]. As illustrated in Fig. 2, the parameters varied for each cell were the tip-curvature radius (ρ) and the rod-electrode angle (θ). The tuning procedure began by setting the curvature radius equal to r_0 and gradually decreasing θ from 40° to 15°. If the resonant frequency did not reach 100 MHz at θ = 15°, the curvature radius was further reduced from r_0 until resonance at 100 MHz was achieved. Through this iterative procedure, a rod-electrode geometry providing uniform capacitance for all cells was obtained.

Based on the results of the RFQFISH analysis, Fig. 3 shows the relationship between the rod-electrode curvature radius and the longitudinal beam position, together with the RFQ tip angle. The average aperture radius is also included in the same figure. The normalized curvature radius of the rod electrodes (ρ/r_0) decreases monotonically from 1 to 0.78 from the entrance up to the 110th cell (z ≈ 1240 mm) and then increases toward the downstream end. In contrast, the tip angle θ decreases monotonically from 45° to 15° within the first 15 cells and remains constant at 15° in the downstream region. The width of the rod-electrode base is 15 mm, and the distance from the base to the beam axis is 23.87 mm. The resonant frequency evaluated at the average aperture radius for all cells remains within 100 ± 0.02 MHz. These results indicate that appropriate adjustment of the curvature radius and tip angle in each cell enables the design of variable-aperture rod electrodes that maintain both a uniform electric-field distribution and a stable resonant frequency.

The influence of cell-to-cell variations in the electrode-tip curvature radius on RFQ beam transmission was evaluated by means of beam dynamics simulations. The simulations were performed using TraceWin and Toutatis [23]. The electric-field distribution was generated from the cell parameters shown in Fig. 1, incorporating the curvature radii obtained in the previous section. The corresponding rod-electrode geometry was constructed, and the field map was calculated in Toutatis by solving the Poisson equation. The accelerated ion species was Li^{3+} with a

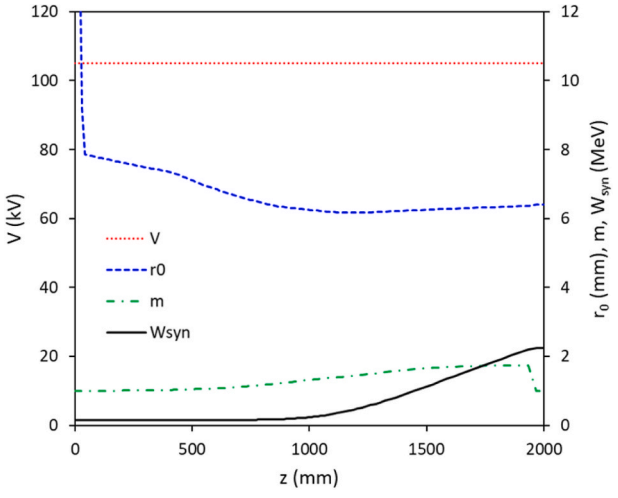

Fig. 1. Cell parameters of the variable-aperture four-rod RFQ linac for longitudinal positions. (Inter-vane voltage: V, Average aperture radius: r0, Modulation index: m, Synchronous Energy:Wsyn).

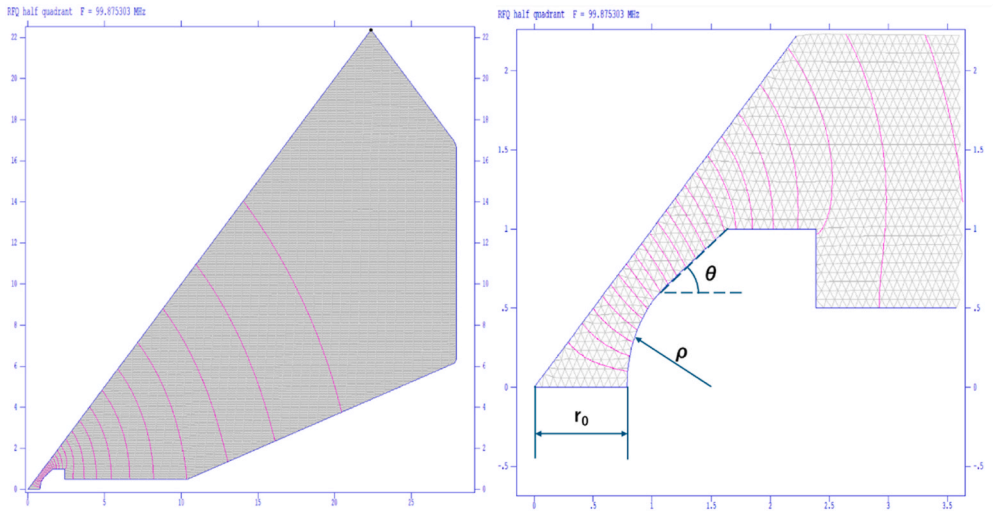

Fig. 2. Simulation model of the cross-sectional shape of the 2D rod electrode by RFQFISH.

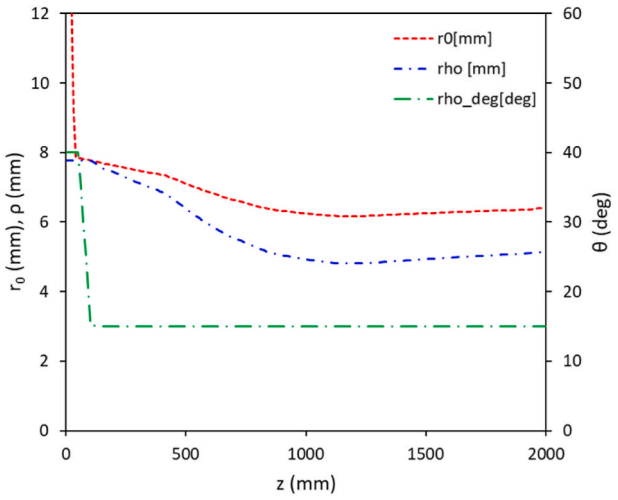

Fig. 3. Tip angle (θ) and curvature radius of the rod electrode relative to longitudinal positions.

beam current of 200 mA. A total of 10,000 macroparticles were tracked, assuming a Gaussian input distribution. The injection energy was 21.8 keV/u, and the input emittance and Twiss parameters were identical to those used in the PARMTEQM calculations. At the nominal inter-electrode voltage of 105 kV, the Toutatis simulation yielded a beam-transmission efficiency of 76.72 % (153.44 mA). Although this value is 2.28 % higher than that obtained with PARMTEQM, the results indicate that the cell-to-cell variations in the electrode-tip curvature radius do not cause any significant degradation of RFQ beam-transmission performance.

2.2. Simulation of 3D electromagnetic field

Based on the curvature radius and tip angle of the rod electrodes obtained from the two-dimensional electromagnetic field analysis for each cell, a three-dimensional CAD (3D-CAD) model of the variable-aperture rod electrodes was constructed. The (ρ, θ) values calculated with RFQFISH, which satisfy the condition of equal capacitance among all cells, were used to generate the rod geometry along the longitudinal direction with a step size of 0.2 mm. Since the average aperture radius r_0 varies from cell to cell, both r_0 and (ρ, θ) were linearly interpolated near the cell boundaries to ensure geometric continuity and manufacturability of the electrode profile. A SolidWorks macro [24] was employed to generate cross-sectional sketches of the rod electrodes at 0.2 mm intervals, which were then integrated using the loft function to form the complete 3D-CAD model. In the radial matching section (RMS), the curvature radius and tip angle of the electrodes were set to 7.77 mm and 40°, respectively. The constructed rod electrodes were incorporated into a 3D-CAD model of the four-rod RFQ linac, as shown in Fig. 4, and electromagnetic field analyses were performed using CST Microwave Studio (MWS) [25]. For comparison, the electric-field distribution was also evaluated using CST EM Studio (EMS), assuming a uniform inter-electrode voltage of 105 kV. AT the CST MWS, the designs of the stem electrodes and base plate followed those of the four-rod RFQ linac used in the BNL DPIS test bench.

The electric-field distributions obtained using the CST MWS eigenmode solver for the first quadrant are shown in Fig. 5. The electric field was evaluated at positions located 5 mm from the beam axis with a 45° angular offset within the first quadrant. For comparison, each electric-field distribution was normalized to its maximum value. In Fig. 5, the blue curve represents the electric-field distribution calculated using the CST MWS eigenmode solver, while the red curve shows the distribution obtained from electrostatic field simulations using CST EMS. In this analysis, the variable-aperture RFQ linac was designed to maintain a constant inter-electrode voltage of 105 kV across all cells; therefore, the electric-field distribution computed using CST EMS represents an ideal reference. The results show that the electric-field distributions calculated using CST MWS and CST EMS are in good agreement, with a maximum difference of 4.7 % observed near the downstream end of the

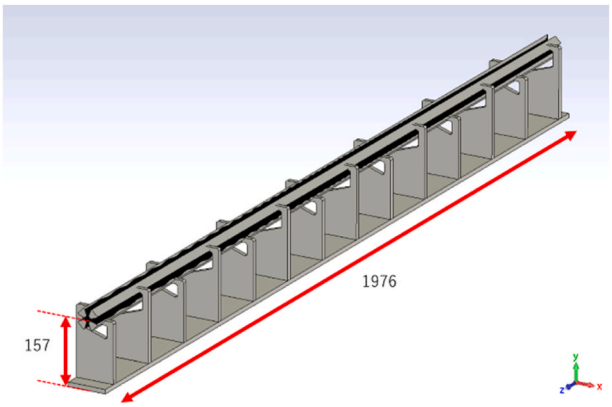

Fig. 4. 3D simulation model of a variable-aperture four-rod RFQ in CST MWS.

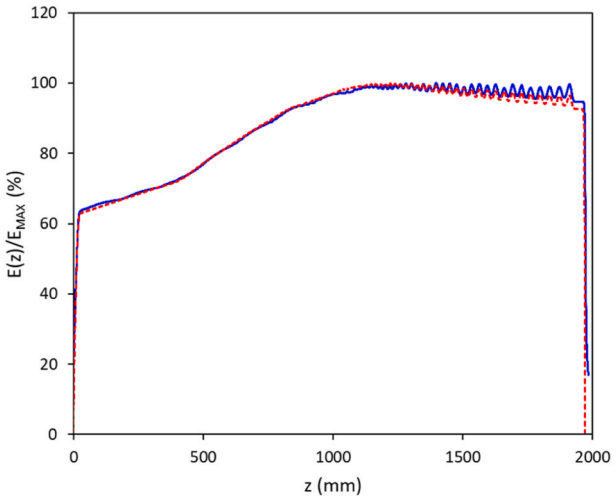

Fig. 5. Electric field distribution along the longitudinal position in the first quadrant. Blue line represents CST MWS for radio-frequency analysis and red line represents CST EMS for electrostatic field analysis. (For interpretation of the references to colour in this figure legend, the reader is referred to the Web version of this article.)

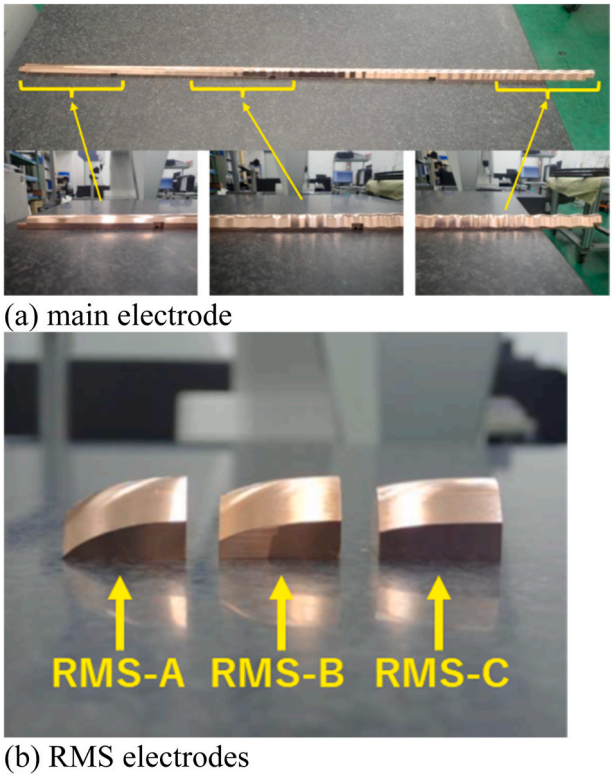

Fig. 6. Pictures of variable-aperture four-rod electrodes: (a) main electrode and (b) RMS electrodes.

structure.

The resonant frequency, unloaded Q value, and maximum surface electric-field strength of the variable-aperture four-rod RFQ linac are summarized in Table 2. The calculated resonant frequency is 94.86 MHz. For comparison, the corresponding four-rod RFQ linac incorporating constant-aperture rod electrodes for Li^{3+} acceleration exhibits a resonant frequency of 94.99 MHz, resulting in a difference of 0.11 MHz. Furthermore, when the nominal inter-electrode voltage is applied, the maximum electric-field strength reaches 24.8 MV/m and occurs between a rod electrode and an oppositely biased stem electrode.

Table 2
Beam parameters of the four-rod variable-aperture RFQ linac.

Resonant frequency	94.86 MHz (94.99 MHz)
Unloaded Q value	3324.3
E_{max} (Kilpatrick factor)	≦24.8 MV/m (2.18 kilp)

3. Fabrication of a variable-aperture four-rod RFQ linac and low-power RF measurements

3.1. Fabrication of the four-rod electrodes

The rod electrodes were manufactured according to the design described in Section 2 using a three-axis vertical machining center (See Fig. 6). Oxygen-free copper (C1020, purity: 99.99 %) was selected for its favorable thermal and electrical properties. The total length of the rod electrodes is 1980 mm and is divided into three sections: the radial matching section (RMS), an upstream main section, and a downstream main section. The RMS incorporates an interchangeable mechanism that allows replacement of electrodes with different geometries, thereby facilitating effective beam matching with the DPIS-type laser ion source and accommodating a range of beam parameters and acceleration conditions. The machining process employed a three-dimensional ball-end mill following a reciprocating tool path along the longitudinal modulation of the rod electrodes. The modulation profile was defined at 0.2 mm intervals along the longitudinal axis, and the ball-end mill machined straight segments between successive points. The butt-joint interfaces between rod-electrode sections were machined on the same fixture to minimize step discontinuities. To ensure the required surface quality, the electrode tips were precisely machined to achieve a transverse surface roughness of less than 1S (Ra ≈0.01 μm) and a longitudinal surface roughness of less than 3S (Ra ≈0.03 μm), where Ra denotes the arithmetic average roughness. The dimensions of the fabricated rod electrodes were verified using a three-dimensional coordinate measuring machine, confirming that they are within ±0.05 mm of the design specifications.

The fabricated rod electrodes were integrated into a four-rod RFQ linac, as shown in Fig. 7. The original four-rod RFQ linac was developed for DPIS through a collaboration between Prof. Schempp at Goethe University Frankfurt and Brookhaven National Laboratory (BNL) and features a vacuum chamber with a total length of 2 m. Vacuum ports are installed at two locations, upstream and downstream, while the RF coupler and tuner ports are positioned at the center along the longitudinal axis of the vacuum chamber. The base plate has a total length of 1976 mm, and the distance from its upper surface to the beam axis is 157 mm. Thirteen stem electrodes are employed, with the 6th and 7th stems designed to be twice as thick as the others in order to connect the upstream and downstream sections of the rod electrodes. Tuner blocks are installed between adjacent stem electrodes, allowing adjustment of the local inductance by varying their height. This configuration enables optimization of both the resonant frequency and the longitudinal distribution of the electric-field strength along the rod electrodes. The four-rod RFQ linac uses the same tuner-block configuration as the constant-aperture four-rod RFQ linac previously employed for Li^{3+} beam acceleration.

3.2. Low-power RF measurement and electric field tuning

To determine the inter-vane voltage distribution between the rod electrodes and the resonant frequency of the constructed variable-aperture four-rod RFQ linac, low-power RF measurements were performed using the perturbation method. Owing to the uniform width (15 mm) of the rod base, the conventional perturbation technique is applicable for evaluating the inter-vane voltage distribution. As an initial step, the perturbation method was applied to assess the inter-vane

(a) four-rod RFQ linac

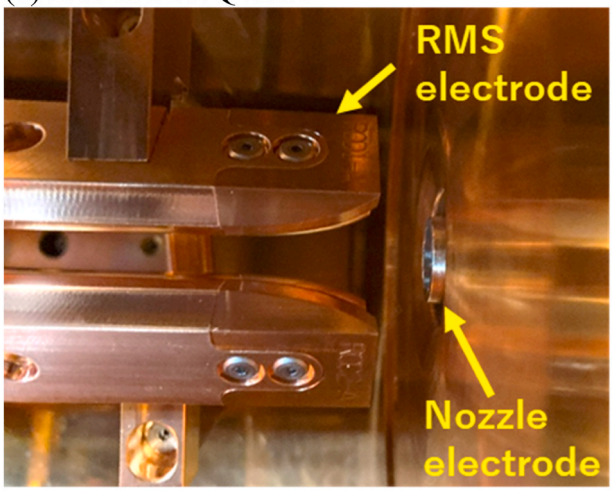

(b) RMS and nozzle electrodes

Fig. 7. Configuration of the four-rod RFQ linac with the new variable-aperture rods for DPIS: (a) four-rod RFQ linac and (b) RMS and nozzle electrodes.

voltage distribution and to validate the electric-field measurements in the variable-aperture four-rod RFQ linac. A polytetrafluoroethylene block was placed as a dielectric perturbing object on the rod electrodes at the midpoint between adjacent stem electrodes, and the corresponding resonant frequency was measured. The inter-vane voltage was then calculated from the measured frequency shift using Eq. (4).

$$(f - f_0)/f_0 \propto -V^2 \tag{4}$$

Here, the resonant frequency measured with the perturbing object inserted is denoted by f, whereas f_0 represents the resonant frequency measured without the perturbing object. Fig. 8 shows the electric-field distribution calculated by simulating the perturbation method with CST MWS. For comparison, the voltage at the same points without a perturbing object were also simulated. or comparison, the electric-field distribution at the same locations without the perturbing object was also calculated. The field values were evaluated at positions corresponding to the center of the perturbing body. Owing to the unique geometric relationship between adjacent stem electrodes at the entrance and exit ends, these regions were excluded from the calculation. The electric-field distribution derived from the perturbation method differs by less than 1 % from that calculated directly using CST MWS. These results confirm the feasibility of measuring the electric-field distribution using the perturbation method in a variable-aperture four-rod RFQ linac.

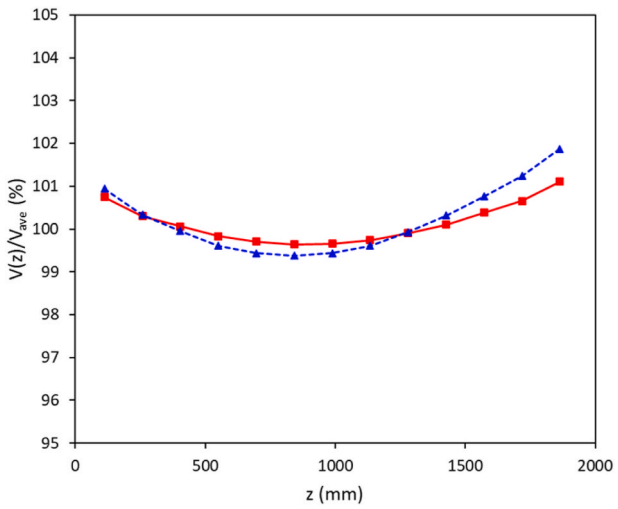

Fig. 8. Inter-vane voltage distribution along the longitudinal position. Blue and red dots represent electric field strength distribution obtained through simulation and perturbation method, respectively. (For interpretation of the references to colour in this figure legend, the reader is referred to the Web version of this article.)

Fig. 9 illustrates the measurement positions for the electric-field distribution obtained using the perturbation method. A polytetrafluoroethylene block (dimensions: 13 × 24 × 111 mm) was used as the dielectric perturbator and positioned in the first quadrant. The 13-mm-wide perturbator was placed at the midpoint between adjacent stem electrodes, with a longitudinal measurement step of 146 mm. The resonant frequency at each measurement position was measured using a network analyzer, and the corresponding inter-vane voltage distribution was determined from the measured frequency shifts using Eq. (4).

The inter-vane voltage distribution of the variable-aperture four-rod RFQ linac measured using the perturbation method is shown in Fig. 10. The distribution exhibits a variation of ±3.8 %. For comparison, the constant-aperture rod previously used for Li^{3+} beam acceleration shows an inter-vane voltage variation of ±1.5 %. This level of uniformity is considered sufficient for the initial state prior to fine tuning. Relatively higher inter-vane voltages are observed at Positions 1 and 13, which can be attributed to the larger transverse cross-sectional area and the resulting higher capacitance of the variable-aperture rod electrodes compared with those of the constant-aperture design.

Subsequently, the base plates were adjusted to improve the uniformity of the inter-vane voltage distribution in the variable-aperture four-rod RFQ linac. The resulting inter-vane voltage distribution is shown in Fig. 11. After several tuning iterations, the variation in the inter-vane voltage distribution was reduced to within ±1.1 %. This result demonstrates that the conventional electric-field tuning method can be effectively applied to a variable-aperture four-rod RFQ linac.

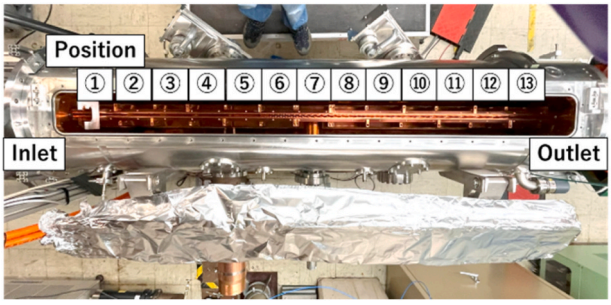

Fig. 9. Measurement position of inter-vane voltage distribution obtained using the perturbation method.

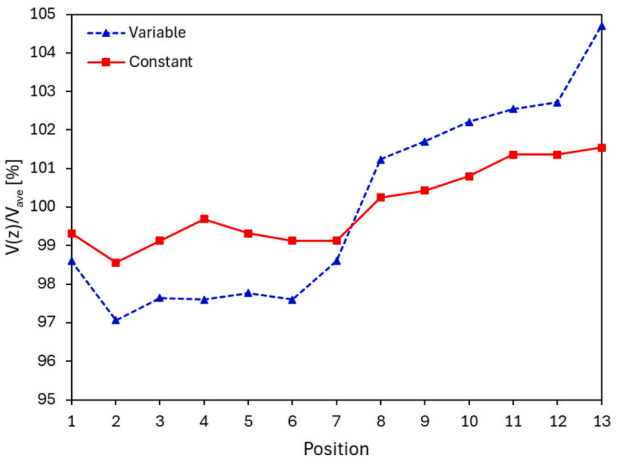

Fig. 10. Inter-vane voltage distributions measured using the perturbation method for the longitudinal position.

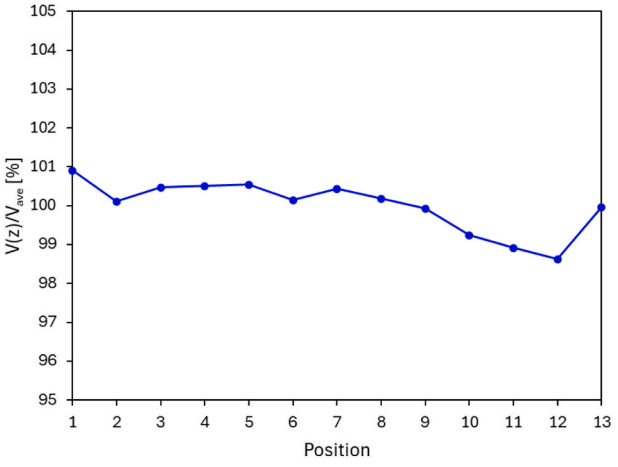

Fig. 11. Inter-vane voltage distribution of the variable-aperture four-rod RFQ linac after tuning the base plate.

The inter-vane voltage distributions obtained with different RMS electrodes are shown in Fig. 12. As the RMS electrode aperture size decreases (RMS-A → RMS-B → RMS-C), slightly higher inter-vane voltages are observed at Positions 1 and 2. This behavior can be attributed to the increased capacitance of the RMS electrodes associated with the reduced aperture size. Based on the inter-vane voltage distribution measured for the constant-aperture rod electrodes (Fig. 10, red symbols), the observed level of variation is not expected to have a significant impact on subsequent beam-acceleration experiments.

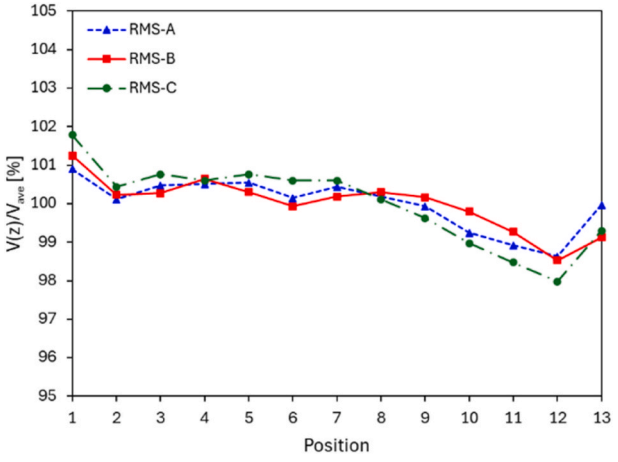

Fig. 12. Inter-vane voltage distributions of the variable-aperture four-rod RFQ linac with each RMS electrode.

The RF properties of the variable-aperture four-rod RFQ linac determined through low-power RF measurements are summarized in Table III. The measured resonant frequency is 99.97 MHz, and the unloaded Q value is 2694. The measured unloaded Q corresponds to approximately 81 % of the value obtained from electromagnetic field simulations. Furthermore, calculations of RF power dissipation indicate that, when the nominal inter-vane voltage is applied, the power loss due to wall dissipation amounts to 256 kW.

4. Conclusion

In this study, we developed a design methodology for a variable-aperture four-rod RFQ linac that maintains a stable electric field distribution behind the electrodes, even as the aperture varies along the structure. This was achieved by systematically adjusting the transverse radius of curvature and the tilt angle of the rod-electrode tips in each cell, thereby ensuring uniform capacitance and a consistent inter-electrode voltage. The validity of this approach was confirmed through low-power RF measurements, demonstrating its feasibility for practical implementation.

Results from three-dimensional electromagnetic field simulations and low-power RF measurements show that the variation in the inter-vane voltage distribution between rod electrodes in the variable-aperture four-rod RFQ linac is within ±3.8 %, in good agreement with the simulation results obtained using CST MWS. Furthermore, measurements of the inter-vane voltage distribution performed using the perturbation method indicate that, after adjusting each base plate, the overall variation can be reduced to within ±1.1 %, which sufficiently satisfies the required performance.

While variable-aperture concepts have previously been demonstrated for four-vane RFQs—such as the approach reported in Ref. [18], in which the required voltage distribution is achieved by locally modifying the cavity inductance along the longitudinal direction—the present study addresses a distinct challenge specific to four-rod RFQs. In this work, variable-aperture cell parameters are realized by compensating the local capacitance through rod-electrode shaping while maintaining a constant inter-vane voltage. These results demonstrate that the proposed design method enables the realization of a variable-aperture four-rod RFQ linac that achieves the intended electric field distribution and satisfies the required RF characteristics.

In future work, beam acceleration experiments will be conducted to achieve lithium beam acceleration at currents of approximately 100 mA using the constructed variable-aperture four-rod RFQ linac.

CRediT authorship contribution statement

Shota Ikeda: Writing – original draft, Software, Data curation, Conceptualization. **Shunsuke Ikeda:** Writing – original draft, Software, Conceptualization. **Takeshi Kanesue:** Writing – original draft, Methodology, Conceptualization. **Toshiro Sakabe:** Writing – original draft, Validation, Methodology. **Antonino Cannavo:** Writing – original draft, Resources, Investigation, Conceptualization. **Masahiro Okamura:** Writing – review & editing, Supervision, Project administration,

Table 3
RF properties of the variable-aperture four-rod RFQ linac.

Resonant frequency	99.97 MHz
Unloaded Q value	2694
Expected maximum wall loss	256 kW
E_{max} (Kilpatrick factor)	≦24.8 MV/m (2.18 kilp)

Funding acquisition, Conceptualization. **Kazumasa Takahashi:** Writing – review & editing, Resources, Methodology, Investigation. **Chuan Zhang:** Writing – review & editing, Software, Resources, Conceptualization. **Masashi Masuoka:** Resources, Investigation. **Horana Gamage Madhawa:** Resources, Methodology, Investigation.

Declaration of competing interest

The authors declare the following financial interests/personal relationships which may be considered as potential competing interests: Masashi Masuoka reports a relationship with TIME Co., Ltd. that includes: board membership. If there are other authors, they declare that they have no known competing financial interests or personal relationships that could have appeared to influence the work reported in this paper.

Acknowledgement

The study at Brookhaven National Laboratory was supported by US DOE, Office of Science, under contract DE-SC0012704.

Data availability

The authors do not have permission to share data.

References

[1] I.S. Anderson, C. Andreani, J.M. Carpenter, G. Festa, G. Gorini, C.K. Loong, R. Senesi, Research opportunities with compact accelerator-driven neutron sources, Phys. Rep. 638 (2016) 1.
[2] S. K Mathot, et al., The CERN PIXE-RFQ, a transportable proton accelerator for the machina project, Nucl. Instrum. Methods Phys. Res. Sect. B Beam Interact. Mater. Atoms 459 (2019) 153–157.
[3] T.P. Wangler, RF Linear Accelerators, John Wiley & Sons, Hoboken, 2008.
[4] G.E. Mcmichael, Low beta CW linacs for intense beams, in: 1990 Linac Conference, 1990. Albuquerque.
[5] H. Brown, T. Clifford, S. Giordano, F. Khiari, R. McKenzie-Wilson, M. Puglisi, P. Warner, Design, fabrication, and testing of the BNL radio frequency quadrupole accelerator, in: The Proceedings of the 1984 Linear Accelerator Conference, 1984. Seeheim, Germany.
[6] C.E. Hill, W. Pirkl, M. Vretenar, E. Tanke, A.M. Lombardi, Performance of the CERN Linac 2 with a high intensity proton RFQ, in: The Proceedings of the 1984 Linear Accelerator Conference, 1994. Tsukuba, Japan.
[7] Y. Liu, M. Otani, T. Miyao, T. Shibata, Z. Fang, K. Futatsukawa, Japan T. Ito, T. Morishita, J. Tamura, K. Okabe, K. Moriya, A. Miura, J, Progress of J-PARC linac commissioning, in: 10th International Particle Accelerator Conference, JACoW Publishing, publisher's location), 2019 page numbers.
[8] V.V. Peplov, D. Anderson, R. Cutler, J. Hicks, R. Saethre, M. Wezensky, SNS linac modulator operational history and performance, in: Proceedings of 2011 Particle Accelerator Conference, publisher's name, publisher's location, 2011 page numbers.
[9] H. Vormann, W. Barth, M. Miski-Oglu, U. Scheeler, M. Vossberg, S. Yaramyshev, High current heavy ion beam investigations at GSI-UNILAC, J. Phys.:Conf. Ser. 2420 (2023) 012037.
[10] A. Schempp, U. Ratzinger, R. Tiede, C. Zhang, J. Alessi, D. Raparia, L. Snydstrup, RFQ and IH accelerators for the new EBIS injector at BNL, in: 2007 IEEE Particle Accelerator Conference (PAC), IEEE, publisher's location), 2007, pp. 1439–1441.
[11] K. Zhu, Y.R. Lu, X.J. Yin, Y.Q. Yang, S.L. Gao, Z. Wang, Y. He, G. Liu, X.H. Zhang, Y.J. Yuan, H.W. Zhao, J.W. Xia, C.E. Chen, The beam commissioning of a CW high charge state heavy ion RFQ, Nucl. Instrum. Methods Phys. Res. 794 (2015) 113–121.
[12] M. Okamura, T. Katayama, R.A. Jameson, T. Takeuchi, T. Hattori, N. Hayashizaki, Carbon beam acceleration using a simple injection method into an RFQ, Nucl. Instrum. Methods Phys. Res. B 188 (2002) 216.
[13] M. Okamura, T. Takeuchi, R.A. Jameson, S. Kondrashev, H. Kashiwagi, K. Sakakibara, T. Kanesue, J. Tamura, T. Hattori, Direct plasma injection scheme in accelerators, Rev. Sci. Instrum. 79 (2008) 02B314.
[14] T. Kanesue, Y. Fuwa, K. Kondo, M. Okamura, Laser ion source with solenoid field, Appl. Phys. Lett. 105 (2014) 193506.
[15] M. Okamura, S. Ikeda, T. Kanesue, K. Takahashi, A. Cannavó, G. Ceccio, A. Cassisa, Demonstration of an intense lithium beam for forward-directed pulsed neutron generation, Sci. Rep. 12 (2022) 14016.
[16] C. Zhang, A. Schempp, Beam dynamics studies on a 200 mA proton radio frequency quadrupole accelerator, Nucl. Instrum. Methods Phys. Res. A. 586 (2008) 153.
[17] C. Zhang, Z.Y. Guo, A. Schempp, R.A. Jameson, J.E. Chen, J.X. Fang, Low-beam-loss design of a compact, high-current deuteron radio frequency quadrupole accelerator, Phys. Rev. Accel. Beams 7 (2004) 100101.
[18] Y. Kondo, T. Morishita, R.A. Jameson, Development of a radio frequency quadrupole linac implemented with the equipartitioning beam dynamics scheme, Phys. Rev. Accel. Beams 22 (2019) 120101.
[19] T. Morishita, Y. Kondo, Electromagnetic design and tuning of the four-vane radio frequency quadrupole with nonuniform intervane voltage profile, Phys. Rev. Accel. Beams 23 (2020) 111003.
[20] C. Zhang, Radio-Frequency Quadrupole Accelerators: from Protons to Uranium Ions, Springer Nature, Switzerland AG, 2023.
[21] J.H. Billen, L.M. Young, Poisson Superfish, Los Alamos National Laboratory Report No. LA-UR-96-1834, 1996.
[22] C.Y. Tan, J.S. Schmidt, A. Schempp, Simple lumped circuit model applied to field flatness tuning of four-rod radio frequency quadrupoles, Phys. Rev. Accel. Beams 17 (2014) 012002.
[23] D. Uriot, N. Pichoff, TraceWin: a beam dynamics simulation code, in: Proc. IPAC2015, 2015, pp. 92–94. Richmond, VA, USA.
[24] Solid works. https://www.solidworks.com/.
[25] CST Studio Suite, Computer simulation Technology(CST). https://www.3ds.com/products-services/simulia/.